

## Wave functions and optical cross sections associated with deep centers in semiconductors

M. Jaros\*†

*Department of Physics and Astronomy, University of Massachusetts, Amherst, Massachusetts 01003*

(Received 7 February 1977)

Analytical impurity wave functions associated with deep levels in semiconductors (e.g., GaAs:O, GaP:O) are calculated, using a pseudopotential scheme in which a realistic and convergent model is employed to represent the host-crystal band structure and the impurity potentials. The effects determining the form of the wave function are studied with a view to establishing a relationship between the position of a deep level in the gap and the localization of the wave function. It was found that the localization is not a sensitive function of the impurity energy measured from the nearest band edge. The optical impurity-to-band cross sections involving deep levels are computed as a function of photon energy and temperature. The electron-phonon interaction is taken into account within the strong-coupling model of Huang and Rhys. A relatively simple formula is derived which can be applied to interpret optical cross sections associated with deep centers dominated by a short-range potential. Numerical results are presented for state one and two of GaP:O, and the threshold energies, the magnitude of the Franck-Condon effect, and the temperature dependence are determined. A brief discussion is given of optical cross sections associated with deep centers in GaAs and Si.

### I. INTRODUCTION

Photoexcitation has been widely used with success to study shallow and deep impurities in semiconductors. The main features responsible for this success are the speed, sensitivity, and the spectroscopic character of the technique. In contrast with standard conductivity measurements of the thermal-activation energy of the Hall constant, the optical method provides data for the relevant transition-matrix elements. The spectral distribution of the optical cross section can be determined at a number of photon energies and in a wide range of temperatures. Thanks to the great sensitivity of the technique, the spectral distribution can be accurately assessed over several orders of magnitude. Hence it is possible to study the broadening of the signal due to the electron-phonon interaction in some detail. In brief, the information provided by a well-planned experiment of this kind may yield the position of the impurity level in the forbidden gap, the character and magnitude of the coupling between the impurity and lattice, the properties of the impurity wave function, and the temperature dependence of the impurity level. Accordingly, the method has recently been refined in several directions. For example, the technique of photocapacitance spectroscopy has been developed which allows the deep levels within the space-charge layer of a  $p$ - $n$  junction or Schottky barrier to be studied directly.<sup>1,2</sup> This technique has been demonstrated by Henry and collaborators<sup>3,4</sup> to be a fine tool for the study of deep levels. A quasi-equilibrium spectroscopic method which uses two light sources and a differentiated photocapacitance signal has been developed by White *et al.*<sup>5,6</sup> Grimmeiss *et al.*<sup>7</sup> have pioneered a method which is

based on the fact that the occupancy of an impurity level is not changed during illumination with photons of different energy if the photocurrent is kept constant. As a result of this lively development a great deal of experimental data has been made available. The strong overlap of this information with that provided by related methods, e.g., luminescence, optical absorption, etc., further enhances the value of the above-mentioned efforts. Unfortunately, the interpretation of the experimental data concerning the optical cross section is not always straightforward and a theoretical model is an essential ingredient in any event. Although the processes associated with shallow impurities seem well understood, this is not the case for deep chemical impurities and defects. Indeed, a truly quantitative analysis cannot be hoped for at the present time because our general understanding of the deep level problem is still poor. Yet it may seem desirable to make use of the existing insight and aim at producing a general prescription which would enable us to extract as much information as possible from a given experimental data.

Recently, we have performed calculations of impurity energies associated with chemical impurities<sup>8</sup> and lattice defects<sup>9</sup> in III-V semiconductors. In some cases we also computed the wave functions associated with deep states. In Sec. II we extend this calculation with a view to establishing a relationship between the position of the level in the forbidden gap and the localization of the wave function. In the past the localization of the impurity wave function has been assessed by relating the argument of the exponential "tail" of the wave function to the impurity energy defined with respect to the nearest relevant band edge. As a result the localization becomes a sensitive function of the position of the

impurity level in the gap. This approach has been shown correct in the case of "shallow" impurities, i.e., those impurities whose nature is determined by a prevailing role of the long-range Coulomb potential. Our calculations indicate that the position of a *deep* state in the gap may not necessarily be a good indication of the degree of localization. This result can be understood if we study the formation of the impurity energy and wave function in terms of the individual contributions associated with various parts of the wave-vector space. In general, numerically significant contributions can be found even from bands lying farther from the principal gap. The position of the impurity level in the gap is a result of a delicate cancellation process in which all these contributions play a part. Consequently, the "depth" of the level is not simply linked to the degree of localization of the corresponding wave function. Since the impurity energy defined in this way is really a difference between large terms of opposite signs, it is not surprising that it is a sensitive function of the strength and symmetry of the impurity potential. The impurity wave function appears to be highly localized and the degree of localization is not so sensitive to the strength of the potential. Both these observations seem useful. In particular, they allow us to simplify calculations of the optical matrix elements. In Sec. III we deal with photoionization cross section  $\sigma_T(h\nu)$  as a function of photon energy  $h\nu$  and temperature  $T$ . The electron-phonon interaction is accounted for within the strong coupling model, in the quasiclassical approximation.<sup>10,11</sup> We arrive there at a simple prescription which allows us to deduce from a set of experimental data the position of the level in the gap, the magnitude of the Franck-Condon effect, the temperature dependence of the impurity level, and to a large degree, also the symmetry of the impurity wave function. In Sec. IV we apply our model to a set of data concerning GaP:O. We also comment on optical properties of similar states in GaAs and Si. We emphasize there the need for studies of temperature dependence of the optical cross sections, without which any data would seem to be incomplete and its interpretation at least to some extent ambiguous.

## II. IMPURITY WAVE FUNCTIONS ASSOCIATED WITH DEEP LEVELS IN SEMICONDUCTORS

Recently, we have reported detailed calculations concerning energy levels associated with "deep" chemical impurities and lattice defects in GaAs and GaP.<sup>8,9</sup> The most obvious aim of such calculations is to predict the positions of the impurity levels in the forbidden gap. Indeed, the impurity energy is often the only observable that is available from experiment. However, with the advance of

various techniques of optical and capacitance spectroscopy some additional data, e.g., carrier capture or photoionization cross sections, is becoming available. In most cases, such an information cannot be processed and made use of in the absence of a reliable description of the impurity wave function. It is, perhaps, characteristic of the state of art in this field that very little is known about the wave functions associated with levels lying further within the band gap. One might expect, as usual in quantum theory, the wave function to be a more sensitive indicator of any inadequacies of a model.

It has been shown in the early days of solid-state theory that the wave functions of the so-called shallow impurities can be thought of as a product of an envelope slowly varying smooth function, and a periodic function derived from the lowest-lying band minima.<sup>12</sup> It was also shown that such an approximation must break down if the dominant part of the impurity potential becomes more localized. If we then expand the impurity wave function  $\psi$  in terms of the complete set of eigenfunctions  $\phi_{n,\vec{k}}$  of the perfect crystal Hamiltonian  $H_0$ ,<sup>13,14</sup>

$$\psi(\vec{r}) = \sum A_{n,\vec{k}} \phi_{n,\vec{k}}(\vec{r}), \quad (1)$$

the coefficients  $A_{n,\vec{k}}$  associated with bands and wave vectors farther from the absolute band minima or maxima may still be numerically significant. [In (1),  $n, \vec{k}$  label bands and reduced wave vectors, respectively.] The simple separation of the impurity wave function into the envelope and periodic parts is no longer possible and the wave function  $\psi$  must be calculated numerically. We can, for instance, compute the impurity energy and coefficients  $A_{n,\vec{k}}$  following the methods of Refs. 8 and 9 and output  $\psi(\vec{r})$  of Eq. (1) at some real space points  $\vec{r}_0$ . As we shall see later, such a procedure reveals some interesting properties of the wave function. However, it might be more convenient to generate  $\psi$  directly in an analytic form as a solution of the Schrödinger equation with the proper Hamiltonian and impurity energy.

It is borne in mind that a small angular variation, and a nodal structure extending far beyond the nearest-neighbor distance may not be relevant if we choose to deal with a deep state of  $A_1(T_d$  group) symmetry.<sup>8,13</sup> Indeed, one expects a carrier with an energy near the middle of the gap to be well localized within the volume comprising the impurity and its nearest neighbors. In such a case only a few parameters may be sufficient to capture the most important features of  $\psi$  and provide a useful analytic function which is well behaved for large values of  $\vec{r}$  and has a correct normalization.

Let us begin by choosing a trial function

$$\psi^0 = a_1 f_1 + a_2 f_2, \quad (2)$$

where

$$f_1 = (N_1)^{-1/2} e^{-\alpha r}, \quad f_2 = (N_2)^{-1/2} (1 + \beta r) e^{-\alpha r}, \quad (3)$$

and define  $\beta$ ,  $N_1$ , and  $N_2$  so as to ensure

$$\int_0^\infty f_i f_j r^2 dr = \delta_{ij}. \quad (4)$$

The function  $\psi^0$  must satisfy the Schrödinger equation

$$(H_0 + h)\psi = \epsilon\psi, \quad (5)$$

where  $h$ ,  $\epsilon$  represent the impurity potential and energy, respectively, and are assumed to be known from our earlier calculations of  $\epsilon$ .<sup>8,9</sup> We may write

$$(H_0 - \epsilon)\sum A_{n,\mathbf{k}} \phi_{n,\mathbf{k}} + h\psi^0 = 0, \quad (6)$$

and substitute for  $\psi^0$  from (2), multiply by  $\phi_{n',\mathbf{k}'}^*$  and integrate to obtain

$$A_{n',\mathbf{k}'} + \sum_{i=1}^2 a_i \frac{\langle \phi_{n',\mathbf{k}'} | h | f_i \rangle}{E_{n',\mathbf{k}'} - \epsilon} = 0. \quad (7)$$

Multiply by  $\langle f_j | \phi_{n,\mathbf{k}} \rangle$ , and  $\sum_{n',\mathbf{k}'}$  gives

$$\sum_{n,\mathbf{k}} A_{n,\mathbf{k}} \langle f_j | \phi_{n,\mathbf{k}} \rangle + \sum_{i=1}^2 a_i \times \sum_{n,\mathbf{k}} \frac{\langle \phi_{n,\mathbf{k}} | h | f_i \rangle \langle f_j | \phi_{n,\mathbf{k}} \rangle}{E_{n,\mathbf{k}} - \epsilon} = 0; \quad (8)$$

the sums can be readily computed following the procedures in Refs. 8 and 9, and the parameter  $\alpha$  can be determined from the condition  $\text{Det}=0$ .<sup>14</sup> Finally, the coefficients  $a_1$ ,  $a_2$  can be calculated and  $\psi^0$  of Eq. (2) rewritten

$$\psi^0 = N^{-1/2} (1 + \gamma r) e^{-\alpha r}. \quad (9)$$

To test the reliability of the wave function  $\psi^0$  defined in (9) we can invoke a consistency condition based on Eq. (6). If we compute a coefficient  $A_{n,\mathbf{k}}^0$  from

$$A_{n,\mathbf{k}}^0 = -\langle \phi_{n,\mathbf{k}} | h | \psi^0 \rangle / (E_{n,\mathbf{k}} - \epsilon), \quad (10)$$

then

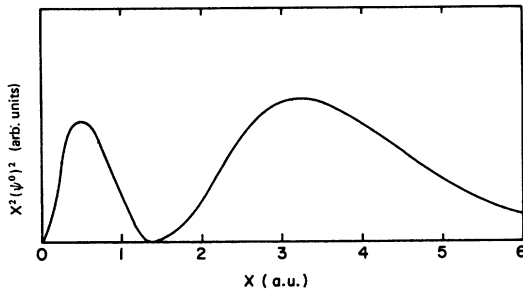


FIG. 1. Sketch of  $x^2(1-0.68x)^2 \exp(-1.72x)$ .

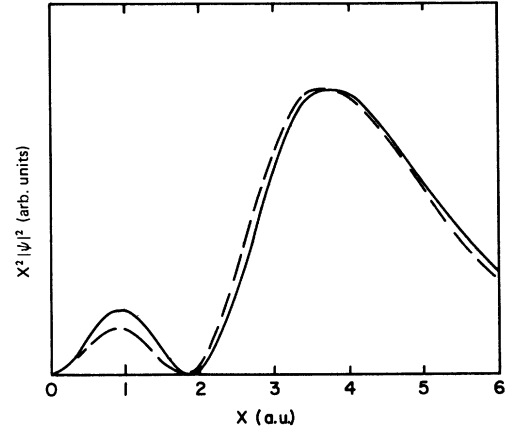


FIG. 2.  $x^2\chi(x)\chi^*(x)$  of Eq. (11) for the trial-function parameters  $\alpha=0.86$ ,  $\gamma=-0.68$  (solid line) and  $\alpha'=0.50$ ,  $\gamma'=-0.55$  (interrupted line).

$$\chi = \sum A_{n,\mathbf{k}}^0 \phi_{n,\mathbf{k}} \quad (11)$$

should be indistinguishable from  $\psi^0$ .

As we indicated earlier our procedure might have the best chance of success if applied to what is basically an s-like state. Calculations of the impurity energies concerning a substitutional donor oxygen in GaP and GaAs have been performed<sup>8</sup> and deep levels obtained. Therefore the above procedure was applied to compute  $\psi^0$  and  $\chi$  for GaAs:O ground state. We find  $\gamma=-0.68$  and  $\alpha=0.86$ , in atomic units (the energy  $\epsilon=0.78$  eV was used in this calculation).  $r^2\psi^0(r)^2$  is sketched in Fig. 1. In Fig. 2 we plot  $x^2\psi^0(x)^2$ . We also show the values obtained with  $\gamma'=-0.55$  and  $\alpha'=0.50$  for comparison.

In Fig. 3 we show  $\chi\chi^*$  for both sets of  $\gamma, \alpha$  to reveal the form near  $|\mathbf{r}| \sim 0$ . Since the details of  $\chi(x)$  are relatively insensitive to the choice of the parameters  $\gamma, \alpha$ , we might ask whether the form of  $\chi$  is at all similar to the form of  $\psi$  introduced via Eq. (1) (i.e., the function obtained via  $A_{n,\mathbf{k}}$ , without the help of a trial function  $\psi^0$ ). When the calculation of  $\psi$  is carried out, it turns out that  $x^2|\psi(x)|^2$  lies in between the two curves shown in Fig. 2 and can be well reproduced from (9)–(11) with a trial function (9) if  $\gamma'=-0.56$  and  $\alpha'=0.69$  a.u.

The difference between  $\alpha' (=0.69)$  and  $\alpha (=0.86)$  may indicate the degree of accuracy of determining the localization of the wave function. In this regard the pessimism of our introductory remark seems well justified. It might be argued that a higher-order polynomial in (9) could improve the situation. Alternatively, we may feel that it is sufficient to determine the wave packet of Eq. (1) at a grid of points in space and fit a polynomial function which describes these points. Naturally, such options

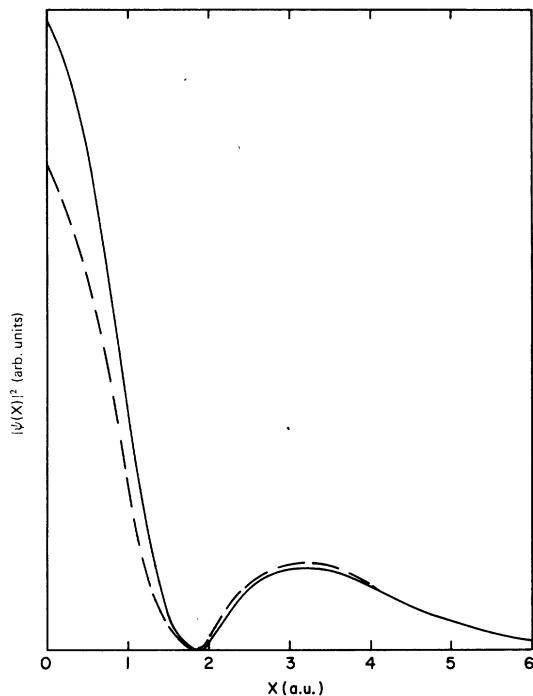


FIG. 3.  $\chi(x) \chi^*(x)$  of Eq. (11) for the two sets of parameters  $\alpha, \gamma$ . Notation as in Fig. 2.

cannot be ruled out since, in principle, they are perfectly straightforward—although tedious prescriptions to follow. However, even for a state of  $A$  symmetry which is being considered here, the angular properties of the wave packet in the region of the second and higher nodes pose problems. Furthermore, the amplitudes of  $|\psi|^2$  in the region of, say,  $r \approx 10$  a.u. are typically by two or three orders of magnitude smaller than  $|\psi(0)|^2$ . The technical requirements which are set by these circumstances seem unreasonable. For example, we would have to aim at less than 1% error in  $\psi$  in order that the small amplitudes at larger  $\bar{r}$  be meaningful at all!

There are several reasons which seem to diminish the importance of the discrepancy brought about by the large difference between  $\alpha$  and  $\alpha'$ . The parametrization chosen in Eqs. (2) and (3) links the parameter  $\alpha$  which appears in the exponential, to the parameter  $\beta$  and consequently to the position of the node. Although this form is computationally convenient, it may impose a constraint upon  $\alpha$ . It can be seen from Figs. 1–3 that the position of the node is always enforced, no doubt at the expense of an increased error in  $\alpha$ .

We can show that the same difference between  $\alpha$  and  $\alpha'$  is found for the two-electron state O in GaP. In Ref. 8 we presented the first-principles wave function [derived via Eq. (1)] for the ground

state of this center. If we apply the procedure of Eqs. (2)–(9) to this case we arrive at  $\alpha = 0.83, \gamma = -0.68$ . A glance at Fig. 1 of Ref. 8 will confirm that the same relationship between the primed and unprimed parameters is found.

Since our early efforts<sup>13</sup> in this field we have repeatedly observed that the localization of the wave function did not change as expected from the change in the position of the level in the gap. The data presented in Ref. 15 are also an eloquent example. The simplest way to demonstrate this effect is to scale the impurity potential, i.e., to multiply it by a suitable constant (the impurity energy of an  $s$ -like state changes quite substantially with scaling<sup>8,9</sup>) and subsequently compute a new wave function. If, for instance, we bring the energy per electron in the above-mentioned two-electron state of GaP:O down from 1.15 to 0.75 eV, the parameters  $\alpha, \gamma$  become 0.79 and  $-0.61$ , respectively.

In the above paragraphs we have emphasized that both the conduction and valence band must be included in the expansion (1) in order that a convergent result for  $\epsilon$  and  $\psi$  be ensured. The convergence properties of the calculation as far as the impurity energy  $\epsilon$  is concerned have been shown in detail.<sup>8,9</sup> It might be of interest to point out that an analogical comparison is possible as far as the wave function is concerned. We can recall our earlier calculation in which the wave functions for<sup>16</sup> GaAs:O and<sup>15</sup> GaP:O were computed with an expansion in Eq. (1) truncated to include effectively only the lowest two conduction bands. In those calculations the technique of solving the Schrödinger equation was somewhat different but the general form of both expansion (1) and the pseudopotential exactly the same. The first node of the wave function  $\psi(x)$  appeared at a larger value ( $\approx \frac{1}{8} a_{\text{lattice}} \sqrt{3}$ ) of  $x$  than that shown in Fig. 2. Also the results from the truncated expansion appear to be less localized. However, the overall character of the wave function is *not* much changed which emphasizes the prevailing role of the conduction bands in the formation of these states.

This important observation can be extended to include states dominated by contributions from valence bands. Our calculations concerning energies and wave functions introduced by lattice defects in GaAs,<sup>9</sup> and also in<sup>17</sup> GaP certainly support this view.

It is borne in mind that if the above conclusions are correct then we can hardly expect the difference in localization of the impurity wave function to help us greatly in distinguishing one impurity from another when we come to relate the localization to the observed spectra. Also there seems to be no substantial change in the nodal character of  $\psi$  as a

function of impurity energy provided that the symmetry is preserved. It is worth emphasizing that so far we have concentrated our attention on defects or deep impurities possessing the high symmetry of a substitutional site in the zinc-blende lattice. Our conclusions cannot be of course automatically extended to interstitials or defects of very low symmetry.

In the past the localization of wave functions associated with levels lying deeper in the gap than the so called shallow donors or acceptors has been estimated from the quantum-defect theory.<sup>18</sup> For example, in their interesting study of the isotope shift for zero-phonon optical transition at traps in semiconductors,<sup>19</sup> Heine and Henry evaluate the probability  $P$  of a carrier being on an atom. To compute  $P$  for deep donor oxygen in GaP, they introduce an envelope function

$$R(r) \sim r^{\nu-1} e^{-r/a}, \quad (12)$$

where  $a = (2m^*E_i)^{-1/2}$  (a.u.). The parameter  $\nu$  is determined by relating the effective mass (hydrogenic<sup>12</sup>) value  $E_H$  for a donor in GaP to the actual value of the impurity energy  $E$ ,

$$\nu^2 = E_H/E_i. \quad (13)$$

For a deep donor like GaP:O,  $\nu \approx (0.05/0.9)^{1/2} \ll 1$  and the envelope function in (12) becomes very similar to the solution of the Schrödinger equation with a  $\delta$ -function impurity potential.<sup>20,21</sup> Our calculations on this subject show quite clearly that a substantial area in the wave-vector space is involved in the formation of the donor ground state and the effective-mass parameter is not applicable in the circumstances. Therefore the localization of the wave function cannot be well represented with the function of Eq. (12). However, the nodal character of the wave function is dominated by the standing waves of the lowest parts of the conduction band as conceived in the quantum defect model. Perhaps as a simple approximation we can still formally write the impurity wave function as a product of a periodic part determined rather well by the nodal properties of the dominating band states and a decaying (localized) function. The precise nature of the latter may be immaterial because it probably does not change strongly enough from defect to defect to be helpful in our analysis of most spectroscopic data.

### III. OPTICAL CROSS SECTIONS

The experimental results of a photoconductivity or optical-absorption study can normally be reduced to a normalized cross section  $\sigma$  per photon, and it is our prime interest to relate this observation to a particular defect or impurity. In practice,

we really want to *distinguish* one curve from another, i.e., the real task is to predict the temperature dependence and the shape of the function  $\sigma_T(h\nu)$  (where  $h\nu$  is the photon energy and  $T$  stands for temperature) in relation to the nature of the impurity concerned. We propose to characterize a deep level by a set of parameters  $E_i$ ,  $E_m$ ,  $d_{FC}$ , and  $\Delta E_T$ .  $E_i$  is the binding energy and is defined as the true energy of the state taking part in the transition, with respect to the edge of a specified band of the host crystal. The maximum of the normalized cross section occurs at a photon energy  $E_m$ .  $d_{FC}$  is the magnitude of the Franck-Condon effect.  $\Delta E_T$  is the shift of the impurity level at  $E_i$  in the gap, caused by a change in temperature. We also desire to determine symmetry properties of the impurity wave function.

Let us first choose to consider the optical cross section associated with an impurity-to-band transition assuming that the electron-phonon interaction is weak and can be left out. Then it is a standard approximation to write

$$\sigma(h\nu) = \frac{\text{const}}{h\nu} \sum_{n, \vec{k}} |\langle \psi | \exp(-i\vec{k}_\lambda \cdot \vec{r}) \vec{\epsilon}_\lambda \cdot \vec{p} | \Phi_{n, \vec{k}} \rangle|^2 \times \delta(E_i + E_{n, \vec{k}} - h\nu). \quad (14)$$

$\vec{k}$  is the wave vector of the radiation field and  $\lambda$  is the polarization direction. In the usual dipole approximation we have  $\exp(-i\vec{k}_\lambda \cdot \vec{r}) \sim 1$ . The momentum matrix element in (14) really indicates an average over all degenerate initial and final states. The band wave functions and energies indicated by  $\Phi_{n, \vec{k}}$  and  $E_{n, \vec{k}}$  must be generated at a large number of points in the Brillouin zone and the expression in (1) evaluated numerically if a truly quantitative answer is required. Also the impurity wave function  $\psi$  is needed as an input in such an exercise. In this application it is convenient to express  $\psi$  as in (1), i.e., via the coefficients  $A_{n, \vec{k}}$ . A calculation along these lines has been performed<sup>8</sup> for a transition from the two-electron state of oxygen in GaP to the conduction band at low temperatures. However, a proposition that such calculations be performed for all cases of interest, is unrealistic. Indeed, as soon as the temperature rises and strong electron-phonon interaction allowed for, the prospect of accomplishing this task disappears from our horizon. On the other hand, the impact of any simplification we make must be carefully assessed. The detailed calculation showed that the sum in (14)—when performed with a highly localized function  $\psi$ —is not a sensitive function of the form of  $\psi$ . The powerful averaging process implied in (14) always leads to a smooth curve for  $\sigma(h\nu)$  and its shape reflects mainly the nodal mismatch between  $\psi$  and  $\Phi_{n, \vec{k}}$ , as well as the variation

in the density of states of the continuum.

In Sec. II we indicated the localization of the impurity wave function associated with a deep state and pointed out that it does not change considerably with impurity energy. This will help to simplify (14). The momentum matrix element in (14) is, with  $\psi$  from (1),

$$\langle \psi | p_\lambda | \Phi_{n,\vec{k}} \rangle = \sum A_{n,\vec{k}}^* \langle \Phi_{n,\vec{k}} | p_\lambda | \Phi_{n,\vec{k}} \rangle. \quad (15)$$

We can rewrite (5) with  $\psi$  from (1), multiply from the left by  $\Phi_{n,\vec{k}}^*$ , and integrate over all coordinates to obtain  $A_{n,\vec{k}}$ ,

$$-A_{n,\vec{k}} = \langle \Phi_{n,\vec{k}} | h | \psi \rangle / (E_{n,\vec{k}} - E_i). \quad (16)$$

Since we generate  $h$ ,  $E_{n,\vec{k}}$ , and  $\Phi_{n,\vec{k}}$  within a pseudopotential scheme, the crystal wave functions are represented by linear combinations of plane waves, i.e.,

$$\Phi_{n,\vec{k}} = \sum_j b_{n,\vec{k}}(\vec{G}_j) \exp[i(\vec{k} + \vec{G}_j) \cdot \vec{r}], \quad (17)$$

where  $\vec{G}$  stands for a reciprocal-lattice vector. The bands  $n$  and the reduced wave vectors  $\vec{k}$  which contribute to the transition probability at a particular photon energy  $h\nu$  are selected by the  $\delta$  function and the optical integral which appear in (14). Because of our declared intention not to get involved in the lengthy business of computing the sum in (14) by a sampling procedure, we must now enter upon the dangerous path of simplifications. Let us choose to represent the band wave functions by those of an isotropic semiconductor.<sup>22,23</sup> Accordingly, the band functions take a form

$$F_k^\pm = (e^{ikr}/\sqrt{2})(C_1 e^{ik_F r} \pm C_2 e^{-ik_F r}), \quad (18)$$

with  $C_1 = C_2 = 1$ , and with + and - referring to the valence and conduction bands, respectively. At the band edge, the band functions are just  $(1/\sqrt{2})(C_1 e^{ik_F r} \pm C_2 e^{-ik_F r})$ .  $\frac{1}{2} k_F^2$  is the free-electron Fermi energy in a.u.

It is easy to show that the Fourier transform indicated by the matrix element in (16) is constant over the range of energies  $E_{n,\vec{k}}$ , over which the mismatch between the nodal character of  $\Phi_{n,\vec{k}}$  and  $\psi$  remains (on average) the same. In Sec. II we concluded that  $\psi$  may be formally written as a product of two terms, one representing the nodal properties of  $\psi$  and the other being a strongly localized function. We may, for instance, write

$$\psi \sim (e^{-\alpha r}/r) F_0^\pm. \quad (19)$$

The analogy with the quantum-defect effective-mass theory is merely in the form since we do not propose to choose  $\alpha$  according to Eq. (12). The nodal part is chosen as a standing wave associated with the relevant band edge. We will return to comment upon this assumption later.

In the case of most deep states, the impurity potential is dominated by its short-range part. The impurity pseudopotential generally derives its strength from the area near the optimized-model potential radius which is typically of the order of the tetrahedral covalent radius  $r_c$ , or less. Therefore, we are not likely to overestimate the localization of  $h$  if we choose  $h \sim r e^{-r/r_c}$ . Then the leading term in the expression for the matrix element in (16) is

$$I(E_{n,\vec{k}}) = \langle \Phi_{n,\vec{k}} | h | \psi \rangle \sim \frac{C_1^2 \pm C_2^2}{k} \times \int_0^\infty \sin(kr) r e^{-ur} dr, \quad (20)$$

where  $u = \alpha + 1/r_c$ . Hence

$$I(E_{n,\vec{k}}) - I_k \sim [u/(k^2 + u^2)^2](C_1^2 \pm C_2^2). \quad (21)$$

In Sec. II, we presented some results concerning the localization of the impurity wave functions associated with deep states. We found that  $\alpha \sim 0.5$  (a.u.). The typical value for  $r_c$  is 2 a.u. so that  $u \sim 1$  a.u. Since the range of photon energies is restricted to  $h\nu \lesssim E(\text{gap})$  (and in fact the ionization energy  $E_i$  constitutes a substantial portion of that energy), the values of  $k^2$  entering (21) appear to be small compared to  $u$ , i.e.,  $I$  is for any practical purposes a constant. It is now easy to see that this result does not really depend upon the choice of a particular analytic form of  $\psi$ ,  $\Phi_{n,\vec{k}}$  since for a somewhat different choice the result would be the same. However, we do need the simplified form of  $\Phi_{n,\vec{k}}$  shown in (18) since it will enable us to eliminate the sampling procedure. Then we can introduce the band density of states  $\rho(E)$  and write (14) as

$$\sigma(h\nu) = \text{const } I \frac{\rho(E)}{h\nu} \left| \frac{\langle F_k^\pm | p | F_k^\pm \rangle (C_1^2 \pm C_2^2)}{E - E_i} \right|^2. \quad (22)$$

Only a transition to a band with nodal properties "matching" those of  $\psi$  is allowed and since  $h\nu = E + |E_i|$ , we arrive at

$$\sigma_L(h\nu) \sim [(h\nu - |E_i|)/h\nu^3] \rho(h\nu - |E_i|). \quad (23)$$

With  $\rho \sim (h\nu - |E_i|)^{1/2}$ , the normalized cross section of (23) has the same form as that of the well-known Lucovsky formula.<sup>20</sup> Had we assumed, as did Lucovsky, that the potential  $h$  in (20) is a  $\delta$  function we would have arrived at  $I = \text{const}$  and consequently Eq. (23) as well. Here we obtain Eq. (23) without having sacrificed much of the realistic form of  $h$  and  $\psi$ . Note that (23) predicts the maximum of  $\sigma(h\nu)$  to occur at  $h\nu = 2|E_i|$ . As we pointed out earlier, our choice to represent the nodal part of  $\psi$ ,  $F_0^\pm$ , in terms of the band-edge standing waves, is merely a convenient vehicle for modeling (at a later stage) the change in the nodal mismatch of the impurity and band wave functions. It means

that we can also observe the "forbidden" transition since in most cases of practical interest  $C_1^2 - C_2^2 \neq 0$ . Hence we arrive at another limiting case, analogous to the Lucovsky formula for our "allowed" transition, i.e.,  $\sigma(h\nu) \sim \rho(h\nu - |E_i|)/h\nu^3$  postulated by Kopylov and Pikhtin.<sup>21</sup>

On our way from Eq. (19) to (22), we kept the mismatch between the nodal structure of  $\psi$  and the band wave function unchanged. Even in the most favorable of circumstances such an assumption becomes invalid when we excite the carrier into states lying farther from the band edge. This is particularly so in the case of the conduction band in direct-gap materials where the importance of the multivalley character of the band structure is manifest. The changes concerning the density of states can be, at least at low temperatures, well accounted for via  $\rho$ . The change in the nodal mismatch, alas, presents an unsurmountable difficulty since its precise rate can only be established by a very detailed calculation. To demonstrate the essence of the problem let us suppose that  $\psi = e^{-\alpha r} \times \Phi_{n_0, \vec{k}_0}/r$ . Then at each sampling point  $n_i, \vec{k}_i$  [chosen in order to evaluate numerically the sum in (14)] the leading contribution to  $I \equiv I(E_{n_i, \vec{k}_i}) \sim M_{n_i, \vec{k}_i}$  where

$$M_{n_i, \vec{k}_i} = \sum_j b_{n_i, \vec{k}_i}^* (\vec{G}_i) b_{n_0, \vec{k}_0} (\vec{G}_i). \quad (24)$$

In evaluating (20) we chose  $\Phi_{n_0, \vec{k}_0}$  and  $\Phi_{n_i, \vec{k}_i}$  in such a way that  $M$  happened to be one or zero. However, the value of  $M$  will fluctuate as we proceed to sample states farther from the band edge. So in general, we must expect a detailed calculation to *reduced the average value of  $I$*  as we increase  $E_{n_i, \vec{k}_i}$ . In the language of our simplified formalism for the evaluation of  $I$ , the average value of  $I_k \sim C_1^2 \pm C_2^2$  where

$$1 \leq C_1^2 + C_2^2 \leq 2 \quad (25)$$

and, for the minus sign,

$$0 \leq C_1^2 - C_2^2 \leq 1. \quad (26)$$

This can be taken into account if we introduce a function  $\eta \equiv \eta(E)$  such that near the band edge  $\eta = 1$  but  $\eta \rightarrow 0$  as  $(h\nu - |E_i|) \rightarrow \infty$ . The cross section then becomes

$$\sigma(h\nu) \sim \frac{\rho(E)}{h\nu} \left| \frac{1 \pm \eta}{E + |E_i|} (E)^{1/2} + \frac{1 \mp \eta}{|E_i| - E_f - E} (E_f)^{1/2} \right|^2. \quad (27)$$

The appearance of the (negative) second term on the right-hand side represents the fact that the wave function  $\psi$  of a deep impurity can now couple to both the conduction and valence band. Formula (27) obviously oversimplifies this relationship. For example the results presented in Ref. 8 show

that only the lowest two valence bands contribute significantly to the totally symmetric ground state of GaP:O. This observation is easy to understand if we recall that the top of the valence band is basically  $p$ -like, whereas the lowest parts of the conduction band are predominantly  $s$ -like. Only the  $s$ -like part of the valence band contributes significantly. Hence, in the language of our isotropic semiconductor model, only the valence states outside the optical gap contribute. We may then change the denominator of the second term to  $|E_i| - \frac{1}{2}E_f - \frac{1}{2}E_p - E$ , where  $E_p$  is the average (Penn)<sup>22,23</sup> gap. It is borne in mind that the degree of cancellation brought about by the appearance of the second term on the right-hand side of (27) depends on the symmetry of the impurity center. By analogy with the states of oxygen in GaP we expect a deep state which is being dominated by the valence bands to have small coefficients  $A_{n, \vec{k}}$  associated with the bottom of the conduction band. Only farther from the edge would the  $p$  character of the band states give rise to a region where  $A_{n, \vec{k}}$  be numerically significant.

In (27) we also assumed that  $k^2/2m^* \equiv E (=h\nu - |E_i|)$  instead of trying to achieve a better balance between  $E^{1/2}$  and  $(E_f)^{1/2}$  by employing some additional corrective parameter. Since this is only relevant for small  $E$  where the second term should not apply in any case, such an addition would not be much of an improvement. However, whatever the precise quantitative form of  $\eta(E)$  and other parameters in (27), the effect upon the shape of  $\sigma(h\nu)$  can only be that the maximum of  $\sigma(h\nu)$  shifts towards *lower* photon energies. We can now understand why the "Lucovsky" form of Eq. (23) so well fits photoionization curves associated with "medium" deep impurities like In in Si [ $E_i \approx 3E_i$  (hydrogenic)] but not those of "shallow" and "deep" impurities. In the case of the shallow impurities the impurity potential is dominated by its long-range Coulomb part and the wave function is very extended. The Fourier transform implied by the matrix element  $I$  is then a sensitive function of  $k$  and its shape depends on the degree of localization of the impurity wave function. As a result the maximum  $\sigma$  occurs at  $h\nu < 2|E_i|$ .<sup>18</sup> For deep levels dominated by a short-range potential,  $2|E_i|$  is a large number, and before  $h\nu$  reaches  $2|E_i|$  the excitations occur from the deep level into the band states lying farther from the band edge. The change in the nodal mismatch leads to a shift of the maximum to  $h\nu < 2|E_i|$ . Although there can hardly be much doubt about the nature of this trend, its quantitative appreciation is difficult to establish. There are obviously many ways of representing  $\eta$  which will in turn affect the precise form of  $\sigma(h\nu)$ .

There is some hope, however, that the actual

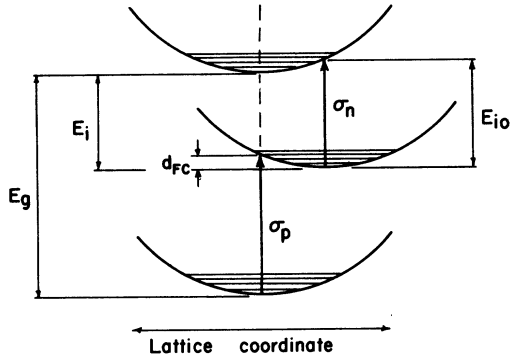


FIG. 4. Configuration-coordinate diagram involving a deep level with binding energy  $E_i$  and the conduction and valence bands separated by a band gap  $E_g$ .  $d_{FC}$  indicates the magnitude of the Franck-Condon effect. The transitions from the level to the conduction band ( $\sigma_n$ ) and from the valence band to the level ( $\sigma_p$ ) are indicated.  $E_{i0}$  is the optical-ionization energy.

form of  $\eta = \eta(E)$  may not be of great significance. We must remember that the sole purpose of introducing this parameter is to take account of the change in the average value of the matrix element  $I$  with  $E$  due to the change in the nodal mismatch of  $\psi$  and the band wave function. Hence  $\eta(E)$  must be a slowly varying function of  $E$ . It should also change very little with temperature. Indeed  $\eta$  must change with  $E$  slowly enough so that the cross sections of medium deep levels are unaffected. Now the minimum gap is always small compared to the average (Penn)<sup>22,23</sup> optical gap  $E_p$  and since  $E_p$  is a good measure of the strength of the crystal potential, the rate of change in  $\eta(E)$  should go as  $\sim (E_p/2)^{-1}$ . Thus we may choose for  $\eta$   $\eta(E) = \exp(-2E/E_p)$  which interpolates smoothly between its apparent values at  $E = 0$  and  $E = \infty$ . Should this prove inadequate  $E_p$  can be used as a free parameter to achieve a better agreement with experiment.

In our discussion of the impurity wave functions associated with deep levels in semiconductors we noted that these functions are highly localized. It is therefore to be expected that when such a state is occupied with an electron, some additional lattice relaxation may take place which significantly changes the position of the level in the gap. It is customary to picture such an effect in a configuration coordinate diagram shown in Fig. 4. The electronic transitions from and into the impurity level, indicated in this figure, reflect the magnitude of this effect (which is connected with the name of Franck and Condon). In the event of strong coupling between the impurity and lattice, the transition probability can be expressed following the model of Huang and Rhys.<sup>24</sup> In this model, the equations for the electronic and phonon functions separate. Only

the electron-phonon interaction which is linear in the lattice coordinates is included. The cross section  $\sigma$  becomes

$$\sigma_T(h\nu) \sim \frac{1}{h\nu} \sum_{n, \vec{k}} |\langle \psi | \exp(-i\vec{k}_\lambda \cdot \vec{r}) \vec{\epsilon}_\lambda \cdot \vec{p} | \Phi_{n, \vec{k}} \rangle|^2 J_{n, \vec{k}}, \quad (28)$$

where the function  $J_{n, \vec{k}}$  carries the information about the vibrational states and for the model in question can be evaluated exactly.<sup>11</sup> At high temperatures and for strong electron-phonon coupling, the expression for  $J_{n, \vec{k}}$  simplifies to

$$J_{n, \vec{k}} \sim (4\pi k_B T S \hbar \omega)^{-1/2} \exp\left(-\frac{(h\nu - [ |E_{i0}^T| + E_{n, \vec{k}} ])^2}{4k_B T S \hbar \omega}\right) \quad (29)$$

Here  $\hbar \omega$  refers to the phonon energy and the term  $S \hbar \omega = d_{FC}$  is shown in Fig. 4.  $k_B$  is the Boltzmann constant.  $E_{i0}$  is the optical-ionization energy of the impurity at  $T$ . The preexponential term obviously does not affect the shape of the optical cross section and for our purposes can be omitted. We may now recall the simplifications which lead us from (14) to (22). Including the expression (29), we rewrite Eq. (28) as follows:

$$\sigma_T(h\nu) \sim \frac{1}{h\nu} \int_0^\infty dE \rho_T(E) \left| \frac{(1 \pm \eta)E^{1/2}}{|E_{i0}^T| + E} + \frac{(1 \mp \eta)(E_F)^{1/2}}{|E_{i0}^T| - E - (E_g + E_p)/2} \right|^2 \times \exp\left(-\frac{(h\nu - [ |E_{i0}^T| + E ])^2}{4k_B T d_{FC}}\right). \quad (30)$$

#### IV. NUMERICAL RESULTS AND DISCUSSION

A glance at Eq. (30) may assure us that had we decided to keep the true band structure in the expression for  $\sigma_T(h\nu)$  [Eq. (14)] we would now have to face an unenviable task of computing the optical sums as many times as necessary in order to accomplish the numerical integration implied in (30). In the light of this observation, we may feel fully justified in having introduced the simplification outlined in Sec. III. Instead of relying on a detailed computer sum evaluation, our simple model describes the changes in the matrix element  $I$  due to the nodal mismatch (between the impurity wave function and the band states of a particular energy) in terms of the parameter  $\eta \equiv \eta(E_p, E)$ . In this study we regard this as the sole purpose of introducing  $\eta$ .  $E_p$  may be, if necessary, treated as a free parameter, together with  $E_{i0}^T$  and  $d_{FC}$ . The computations implied by (30) are minimal and the smallest computer allows them to be repeated as often as required. Hence, a given set of experimental data, i.e., the normalized cross-section



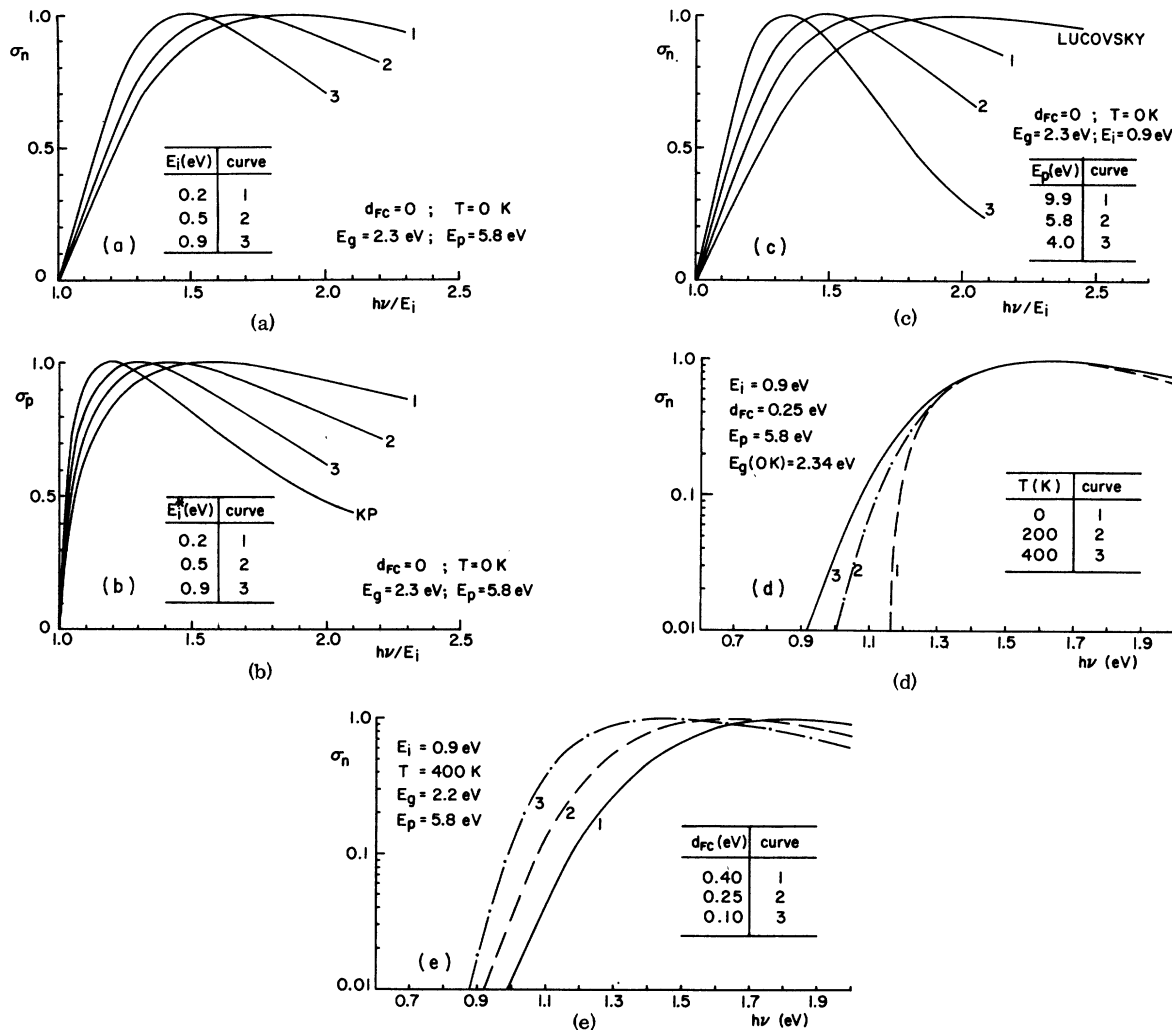


FIG. 5. Normalized cross sections  $\sigma_n, \sigma_p$  for several values of the parameters  $E_i, d_{FC}, E_p$  and temperature  $T$ , from Eq. (28). The nodal properties of the impurity wave function are determined by  $F_0^*$  [Eqs. (18) and (19)]. The relevant values of the parameters are indicated throughout (see also Fig. 4). In (b) the binding energy  $E_i^*$  is measured from the top of the valence band. Note that  $\sigma_L$  (c) and  $\sigma_{KP}$  (b) are the special cases discussed in the text following Eq. (23). The parameter  $E_p$  is introduced and discussed in Sec. III, between Eqs. (23) and (24). Note that  $E_p=5.8$  eV is the average optical gap of GaP. In (d) it is assumed that  $E_i$  is independent of temperature.

curves  $\sigma \equiv \sigma_T(h\nu)$ , at several values of temperature  $T$ , can be interpreted in terms of the optical-ionization energy  $E_{i0}^T$  and the Franck-Condon shift  $d_{FC}$ , fitted to reproduce the data. By selecting  $F_0^+$  or  $F_0^-$  in (18) and (19) which indicates the origin of the nodal character of  $\psi$  and employing (30) we may arrive at a sensitive tool capable of distinguishing cross sections of centers possessing different symmetry properties. In Fig. 5, we summarize some general predictions based on the formula (30). We can see there the shape of the cross sections  $\sigma_n$  and  $\sigma_p$ , associated with transitions from a level to the conduction band and from the valence band to the deep level in the gap, respectively. The notation is consistent

with that in Fig. 4 which shows the transitions in a simple diagram including the Franck-Condon effect parameter  $d_{FC}$ . The effect of temperature upon  $\sigma$  is also demonstrated and it is assumed that the level does not have any temperature dependence (i.e., the binding energy  $E_i$  does not change with temperature). Note that the ambiguity introduced by our somewhat arbitrary choice of the parameter  $E_p$  is not very significant unless  $E_p$  is taken to be much smaller than the average optical gap.

One of the important conditions for a successful interpretation of the experimental data is that the cross-section measurements are taken at several temperatures. It is also essential that the range

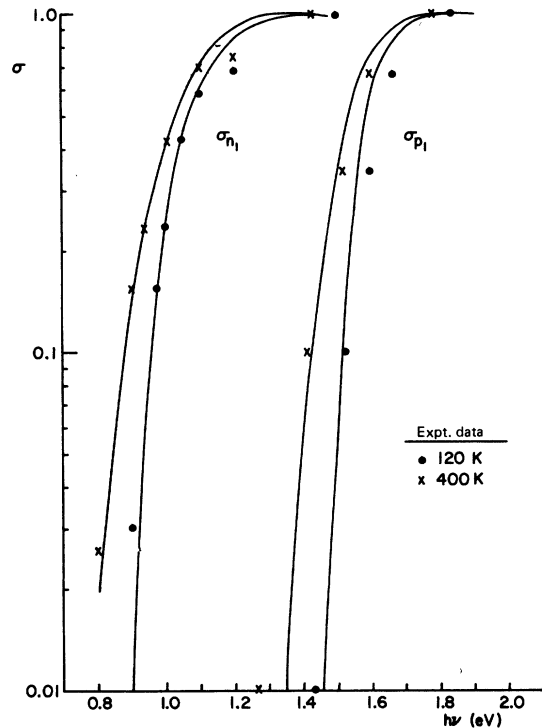


FIG. 6.  $\sigma_{n_1}$  and  $\sigma_{p_1}$  are the transitions from and to the oxygen donor (state 1) ground state [ $E_i$  (4 K) = 896 meV from the conduction band] indicated schematically in Fig. 4. The curves refer to the present calculation with  $d_{FC} = 80$  meV,  $E_i$  (120 K) = 0.87 and  $E_i$  (400 K) = 0.82 eV. The points are the experimental results (Refs. 3 and 26) shown for comparison.

of photon energies covered in the experiment is sufficient to reach both the exponential low-energy tail and the point where  $\sigma(h\nu)$  appears to have a maximum. Should experimental results for  $\sigma_T(h\nu)$  at one temperature only be used for the fit to the formula (30), the result is bound to be ambiguous since in the presence of large Franck-Condon effect there are too many free parameters. With data at different values of  $T$  we might be able to diminish the uncertainty introduced via  $\eta$ .

In Sec. III we proposed that transitions from the valence band to the impurity level be treated in an analogical fashion to those from the level to the conduction band which take place in the area near the  $X$  point. This point is in the center of the Jones-zone flat-surface area.<sup>23</sup> At and near that point our attempt to imitate the "multiband" character of the observed transition by a simple formula in (27) or (30) might be well justified. However, the transitions from the valence band (Fig. 4) occur near the  $\Gamma$  point where the direct (optical) gap is much smaller and the Bragg reflections at higher reciprocal-lattice vectors affect the band wave functions. Our formulas of (27) and (30), if

simply inverted and used to interpret the above-mentioned transitions, must of necessity give a poorer representation of the experimental data.

It is outside the scope of this paper to comment upon the precautions an experimentalist must take in order to generate a trustworthy set of data. Often the photoconductivity data are not supported by any control data (e.g., photo-Hall mobility.) Then, in the absence of any other arrangements, it is not clear whether the observed signal is just a "convolution" representing a number of transitions or whether it corresponds to only one type of transition from one deep level in the gap. In brief, of the vast literature on deep levels only a very small fraction is amenable to theoretical treatment. It goes without saying that the very threshold observed in an experiment is in many cases difficult to establish from data taken at one temperature only. This is particularly apparent in the case of deep levels exhibiting strong coupling to the lattice.

Oxygen in GaP is perhaps the only "deep" impurity as far as III-V semi-conductors are concerned which has been studied extensively enough so that the data required seems available. We will, therefore, concentrate our attention on GaP:O. We will also discuss the applicability of (30) to deep levels in GaAs. Finally, we will discuss some important dopants in silicon, e.g., gold.

#### A. GaP:O—State 1 (one-electron donor state)

The transitions from the donor ground state to the conduction band ( $\sigma_{n_1}$ ) and also the transitions from the valence band to the state in the gap ( $\sigma_{p_1}$ ) have been measured as a function of photon energy and temperature.<sup>3,4,25-28</sup> The experimental points are shown, for  $T = 120$  K and  $T = 400$  K, in Figs. 6 and 7. The band gap of GaP changes from  $\sim 2.32$  to  $\sim 2.22$  eV in this range of temperatures.<sup>29</sup>

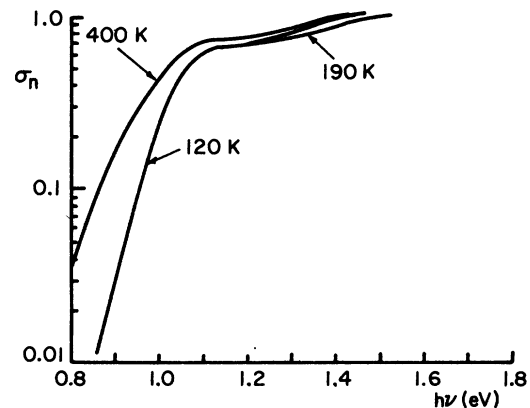


FIG. 7. Plot of the experimental results for  $\sigma_{n_1}$  (GaP:O) at 120, 190, and 400 K (Refs. 3 and 26).

The temperature broadening of  $\sigma_{n_1}$  is relatively small. Taking  $d_{FC} = 0.08$  eV and recalling that the low-temperature binding energy of GaP:O is 0.896 eV (Ref. 30) we arrive at curves shown in Fig. 6 which seem in reasonable agreement with the experimental values. Note that consistent results are obtained for both  $\sigma_{n_1}$  and  $\sigma_{p_1}$ . It transpires that with  $d_{FC} = 80$  meV between 120 and 400 K the oxygen binding energy with respect to the conduction band decreases by 50 meV. The assessment of the temperature dependence is confirmed by the shift of  $\sigma(\text{max})$  as well. The numerical estimate of both figures (80 and 50 meV) is, of course, subject to a large error and these numbers are probably correct only to within  $\pm 10$  meV. The result is in principal agreement with the assessment of Braun and Grimmeiss.<sup>26</sup>

The difference between the observed and calculated cross sections  $\sigma_{p_1}$  is not difficult to accept because of the approximate nature of (30). Also for small  $d_{FC}$  (and/or low temperatures), formula (30) cannot be expected to reproduce faithfully the details of  $\sigma$ . The difference between the calculated and observed  $\sigma_{n_1}$  is more important. To illustrate the effect with greater precision we reproduce the data separately in Fig. 7. The dip in  $\sigma_{n_1}(h\nu)$  starting at  $h\nu \sim 1.15$  eV persists up to high temperatures without any significant change. Therefore, it is not entirely clear whether it can be attributed to a change in the band density of states only. It may be that some other transition is responsible for this odd effect. The point is certainly worth investigating since our understanding of the levels introduced by O in GaP is more advanced than in other cases, where it may serve as a useful (and rare) guide.

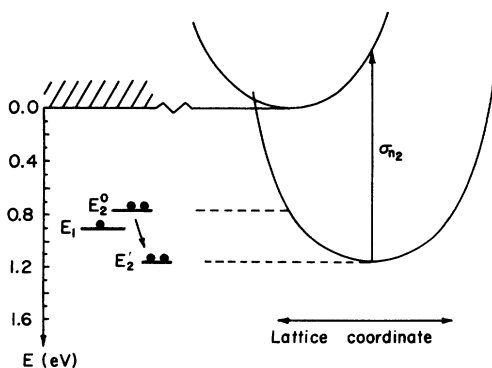


FIG. 8. Summary of computer calculations concerning the two-electron state (state two) of GaP:O (Ref. 8).  $E_1$  is the ground state of the state one. The second electron is captured at  $E_2^0$  and the following lattice relaxation brings the energy per electron down from  $E_2^0$  to  $E_2'$ . The transition of an electron to the conduction band ( $\sigma_{n_2}$ ) is also shown.

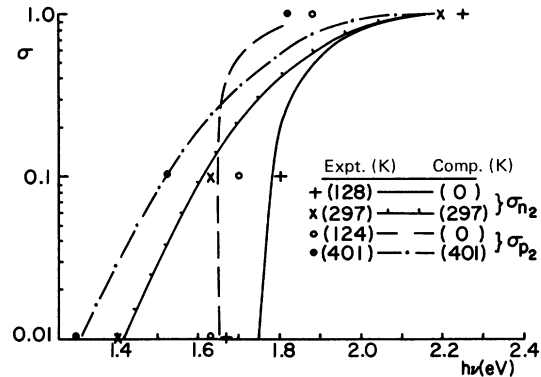


FIG. 9. The computed and experimental (Ref. 3) results for the electron transitions from the two-electron state of GaP:O ( $\sigma_{n_2}$ ) to the conduction band, and from the valence band to the level ( $\sigma_{p_2}$ ). The curves correspond to a Franck-Condon shift of 0.55 eV. The first-principles calculation (Ref. 8) gave 0.4 eV (see Fig. 8).

#### B. GaP:O—State 2 (two-electron state)

The oxygen potential is strong enough to bind two electrons.<sup>8,14,31</sup> The photocapacitance measurements<sup>3,4</sup> were used to extract the optical cross sections  $\sigma_{n_2}(h\nu)$  and  $\sigma_{p_2}(h\nu)$  involving an electron transition from the two electron state to the conduction band and from the valence band to the level in the gap, respectively. The temperature dependence of  $\sigma$  points to a strong coupling to the lattice. A calculation was performed<sup>8</sup> to estimate the magnitude of the change in the electron energy due to lattice relaxation which follows the capture of the second electron and electron charge polarization. That result is pictured in Fig. 8, in terms of a simple configuration coordinate diagram. The shape of  $\sigma_{n_2}$  was also calculated. However, the threshold energy at which this transition should be observed is not easy to deduce from such a calculation, although we know the energy per electron in both, the one and two electron states (and before and after the lattice relaxation takes place), measured with respect to the binding energy of the single donor (i.e.,  $\sim 0.9$  eV). In order to excite one electron from the two-electron state to the conduction band, the energy required to reaccommodate the other electrons in the system must be accounted for. Hopefully this term is small so that  $E_{i0}$  is approximately given by the line shown in Fig. 8. In the present study we can treat  $E_{i0}$  as a function of temperature. A comparison of the present calculation with experiment is shown in Fig. 9. It would appear that the parameter  $d_{FC}$  should be less than 0.55 eV. The above-mentioned computer calculation gave 0.4 eV. The results of our calculations as  $T=0$  and  $T=400$  K, presented in Fig. 9, are compared with the experimental data of Kukimoto

*et al.*<sup>3</sup> The computed curves for  $T=0$  nicely illustrate the dramatic changes brought about by an increase in temperature. An overall agreement in Fig. 9 is good but the shape of  $\sigma_{p_2}$  near its maximum is difficult to understand. However, it must be remembered that these cross sections cannot be easily extracted from the experimental data and the relevant rate equations.<sup>3,4</sup> In a difficult multi-level problem some error is inevitable. Also, our formalism is based on a linear-coupling model which employs only one phonon mode. Nonlinear effects may bring about some additional changes in the shape of  $\sigma_{n_2}$  and  $\sigma_{p_2}$ , and may affect them differently. It would then seem as if the two transitions were effectively associated with a different  $d_{FC}$ , an impression one might get from the comparison in Fig. 9. It is indeed impossible to fit the high-temperature curves well with  $d_{FC}$  being the same for both,  $\sigma_n$  and  $\sigma_p$ .

#### C. GaAs

A single donor substituting for arsenic is expected near the middle of the gap.<sup>3</sup> Experimental data, although in one way or another referring to oxygen, has so far produced no clear confirmation of the prediction. Perhaps because of this uncertainty, and also because of a large number of deep levels present in this material, it is to the best of our knowledge impossible at this stage to gather a set of data equivalent to those for GaP:O. The confusing state of affairs is well documented in recent papers by Lang and Logan<sup>32</sup> or Lin *et al.*<sup>33</sup> A similar situation is characteristic of another important dopant Cr.<sup>34</sup> We will, therefore, make only general comments on the differences we should expect when comparing GaP and GaAs. As we pointed out earlier,<sup>6,35</sup> some effect upon the shape of the cross section  $\sigma_n$  might be expected due to the low density of states area near  $\Gamma$ . We have also indicated that the nearly-free-electron-like model we introduced to allow for a better fit of  $\sigma$  may be

a poor approximation at  $\Gamma$  where the concept of an isotropic semiconductor breaks down. As a result somewhat *sharper* spectra might be expected compared to GaP. However, as in GaP, the data available at present does indicate a number of deep levels in GaAs strongly coupled to the lattice.

#### D. Si

The optical cross sections of several important deep dopants in Si have been measured. The data on deep levels introduced for instance, by Zn,<sup>36</sup> S,<sup>37</sup> Au,<sup>38</sup> and Co (Ref. 39) is customarily interpreted<sup>40</sup> as indicating that none of these impurities exhibits strong coupling to the lattice. This is most remarkable since it might support the old belief that all these may be simple substitutional donors or acceptors. The proposal that gold and cobalt impurities are somewhat related to a complex with vacancy<sup>41</sup> would lead us to anticipate a great deal of lattice relaxation and the temperature dependence of the optical cross sections should show broadening.

Unfortunately, a careful inspection of published material on levels in Si indicates that there are substantial differences between results available in the literature (gold donor being a good example). The complications brought about by the presence of several optically active levels in the material under investigation, and in most cases a restricted range of temperature considered increase the degree of uncertainty. Also the band gap of Si is smaller than that of GaP or GaAs and the absolute changes in the impurity energy are expected to shrink accordingly. We believe, therefore, that under these circumstances the question concerning the lattice relaxation effects in Si remains open.

#### ACKNOWLEDGMENTS

It is a pleasure to thank Claude M. Penchina and Hans J. Stocker for many discussions.

\*Supported in part by ONR under Contract No. N00014-76-0890.

†On leave of absence from Dept. of Theoretical Physics, the University, Newcastle upon Tyne, U.K.

<sup>1</sup>C. T. Sah, L. Forbes, L. L. Rosier, and A. F. Tasch, Jr., *Solid State Electron.* **13**, 759 (1970).

<sup>2</sup>C. T. Sah, W. W. Chan, H. S. Fu, and J. W. Walker, *Appl. Phys. Lett.* **20**, 193 (1972).

<sup>3</sup>H. Kukimoto, C. H. Henry, and F. R. Merritt, *Phys. Rev. B* **7**, 2486 (1973).

<sup>4</sup>C. H. Henry, H. Kukimoto, G. L. Miller, and F. R. Merritt, *Phys. Rev. B* **7**, 2499 (1973).

<sup>5</sup>A. M. White, P. Porteous, and P. J. Dean, *J. Electron. Mater.* **5**, 91 (1976).

<sup>6</sup>A. M. White, P. J. Dean, and P. Porteous, *J. Appl. Phys.* **47**, 3230 (1976).

<sup>7</sup>H. G. Grimmeiss and L.-Å. Ledebø, *J. Appl. Phys.* **46**, 2155 (1975).

<sup>8</sup>M. Jaros, *J. Phys. C* **8**, 2455 (1975).

<sup>9</sup>M. Jaros and S. Brand, *Phys. Rev. B* **14**, 4494 (1976).

<sup>10</sup>K. Huang and A. Rhyss, *Proc. R. Soc. A* **204**, 406 (1950).

<sup>11</sup>T. H. Keil, *Phys. Rev.* **140**, A601 (1965).

<sup>12</sup>W. Kohn, *Solid State Phys.* **5**, 257 (1957).

<sup>13</sup>M. Jaros and S. F. Ross, *J. Phys. C* **6**, 3451 (1973); and also S. F. Ross, Ph.D. thesis (Newcastle University, U.K., 1975) (unpublished).

<sup>14</sup>Note that  $\sum A_{n,\vec{k}} \langle f_j | \phi_{n,\vec{k}} \rangle = a_j$  and we have two homogeneous equations with unknown coefficients  $a_1$  and  $a_2$  to solve. The sums involving the matrix elements of  $h$  are then evaluated with different values of the wave-function parameter  $\alpha$  until the usual condition  $\text{Det}=0$  is satisfied.

- <sup>15</sup>M. Jaros and S. F. Ross, *Proceedings of the Twelfth International Conference on the Physics of Semiconductors* (Teubner, Stuttgart, 1974), p. 401.
- <sup>16</sup>S. F. Ross and M. Jaros, *Phys. Lett. A* 45, 355 (1973).
- <sup>17</sup>M. Jaros and G. P. Srivastava (unpublished).
- <sup>18</sup>H. B. Bebb, *Phys. Rev.* 185, 1116 (1969).
- <sup>19</sup>V. Heine and C. H. Henry, *Phys. Rev. B* 11, 3795 (1975).
- <sup>20</sup>G. Lucovsky, *Solid State Commun.* 3, 299 (1965).
- <sup>21</sup>A. A. Kopylov and A. N. Pikhtin, *Fiz. Tverd. Tela* 16, 1837 (1974) [*Sov. Phys.-Solid State* 16, 1200 (1975)].
- <sup>22</sup>D. R. Penn, *Phys. Rev.* 128, 2093 (1962); J. A. Van Vechten and J. C. Phillips, *Phys. Rev. B* 2, 2160 (1970).
- <sup>23</sup>V. Heine and R. O. Jones, *J. Phys. C* 2, 719 (1969).
- <sup>24</sup>K. Huang and A. Rhys, *Proc. R. Soc. A* 204, 406 (1950).
- <sup>25</sup>G. Björklund and H. G. Grimmeiss, *Solid State Electron.* 14, 589 (1971).
- <sup>26</sup>S. Brown and H. G. Grimmeiss, *Solid State Commun.* 12, 657 (1973).
- <sup>27</sup>H. C. Henry and D. V. Lang, *Phys. Rev. B* (to be published).
- <sup>28</sup>D. V. Lang and C. H. Henry, *Phys. Rev. Lett.* 25, 1525 (1975).
- <sup>29</sup>C. D. Thurmond, *J. Electrochem. Soc.* 122, 1133 (1975).
- <sup>30</sup>P. J. Dean, C. H. Henry, and C. J. Fosch, *Phys. Rev.* 168, 812 (1968).
- <sup>31</sup>S. T. Pantelides, *Solid State Commun.* 14, 1255 (1973).
- <sup>32</sup>D. V. Lang and R. A. Logan, *J. Electron. Mater.* 4, 1053 (1975).
- <sup>33</sup>Alice L. Lin, E. Omelianovski, and R. H. Bube, *J. Appl. Phys.* 47, 1852 (1976).
- <sup>34</sup>Alice L. Lin and R. H. Bube, *J. Appl. Phys.* 47, 1859 (1976).
- <sup>35</sup>M. Jaros, *J. Phys. C* 8, L264 (1975).
- <sup>36</sup>J. M. Herman III and C. T. Sah, *J. Appl. Phys.* 44, 1259 (1973).
- <sup>37</sup>T. H. Nigh and C. T. Sah, *Phys. Rev. B* 14, 2528 (1976).
- <sup>38</sup>S. Braun and H. G. Grimmeiss, *J. Appl. Phys.* 45, 2658 (1973); O. Engström and H. G. Grimmeiss, *Appl. Phys. Lett.* 25, 413 (1974); D. C. Wong and C. M. Penchina, *Phys. Rev. B* 12, 5840 (1975).
- <sup>39</sup>C. M. Penchina and J. S. Moore, *Phys. Rev. B* 9, 5217 (1974).
- <sup>40</sup>D. V. Lang, *Proceedings of the International Conference on Radiation Effects in Semiconductors*, Dubrovnik, Yugoslavia, Sept. 1976 (unpublished).
- <sup>41</sup>J. A. Van Vechten and C. D. Thurmond, *Phys. Rev. B* 8, 3539 (1976).